Low frequency excess noise source investigation of off-diagonal GMI-based magnetometers

Basile Dufay, Elodie Portalier, Sebastien Saez, David Menard, Christophe Dolabdjian, Djamel Seddaoui, Arthur Yelon

Low frequency excess noise source investigation of off-diagonal GMI-based magnetometers

B. Dufay*, E. Portalier*, S. Saez*, C. Dolabdjian*, D. Seddaoui†, A. Yelon†, D. Ménard†,
*Groupe de recherche en Informatique, Image, Automatique et Instrumentation de Caen Normandie Univ, UNICAEN, ENSICAEN, CNRS, GREYC, 14000 Caen, France
†Polytechnique Montréal, Département de génie physique & Regroupement québécois des matériaux de pointe, Montréal, Québec, Canada H3C3A7

***Abstract*—The equivalent magnetic noise spectral densities of off-diagonal GMI based magnetometers exhibit significant low frequency excess noise, proportional to $1/f$ noise. As it represents a serious limitation to the ultimate sensing performances of high sensitivity magnetometers, possible sources of this $1/f$ noise are under investigation. Low frequency magnetization fluctuations have been proposed as the noise source in the case of classical GMI-based sensors. Here, we apply this model to off-diagonal GMI-based magnetometers. This requires the inclusion of magnetization fluctuation noise sources, in addition to white noise sources from electronic conditioning in the GMI effect equations. A pessimistic scenario is presented, predicting the upper limit of low frequency excess noise from material characteristics. The equivalent magnetic noise level is then computed from the sensitivity of each term of the sensing element impedance matrix to the magnetization angle at the static working point (for both axial and circumferential static magnetic field) and to conditioning circuitry. Based on this, it appears that magnetization fluctuations similarly affect all modes of operation of the two-port network sensing element, inducing identical impedance fluctuations. It also appears that this noise depends only upon the static equilibrium condition. This condition is governed by the effective anisotropy of the magnetic wire and by both axial and circumferential static components of the working point.**

***Index Terms*—magnetometer, off-diagonal GMI, magnetic noise.**

I. Introduction

In recent decades, the Giant MagnetoImpedance (GMI) effect has attracted considerable attention due to its considerable potential in high sensitivity magnetometry [1], [2], [3]. It describes the impedance change of a ferromagnetic conductive material due to variation of a magnetic field, applied along the same axis as the current flow. In such a case, the ultimate sensing performance of the sensor is given by its equivalent magnetic noise level, expressed in $\mathrm{T}/\sqrt{\mathrm{Hz}}$.

In most cases, the output noise spectral density can usually be separated into a low frequency, excess, $1/f$, noise, and a white noise floor [4], [5], [6], [7]. As highlighted in previous work [8], the white noise floor is mostly limited by the electronic conditioning noise level. Consequently, it will be advantageous to increase the voltage sensitivity of the sensing element until the electronic conditioning noise and the sensor noise become comparable. One approach to improvement of the sensitivity is the choice of a two-port network configuration, in which the GMI element is associated with a pick-up coil (this is sometimes referred to as off-diagonal GMI [9] or orthogonal flux-gate in the fundamental mode [10], [5]). A white noise model and expected performance of such a sensor have been presented in [6], [8].

In the earlier work, the low frequency excess, $1/f$, noise was not investigated even though it represents a non-negligible part of the output equivalent magnetic noise spectral density. We have recently proposed [11] low frequency magnetization fluctuations as a possible source for such noise, and have developed a model for a sensor based on a classical GMI device (without pick-up coil). Here, we extend this low frequency excess noise model to the other possible cases of a two-port network sensing element, including the off-diagonal case. This extension relies upon general equations for the GMI effect, allowing us to analyze the effect of working conditions on the noise behavior.

The paper is organized as follows. Section II recalls the theoretical basis of a GMI based sensor operation. Section III is dedicated to noise sources, including both white and low-frequency excess noise. Results and discussion are presented in section IV, and followed by a general conclusion.

II. Principle of the sensing element

As previously described, we consider a sensing element consisting of a pick-up coil wound on an amorphous ferromagnetic wire exhibiting GMI effect [8]. In the linear regime, this sensing element is fully described by its field-dependent impedance matrix:

$$\begin{pmatrix} v_1 \\ v_2 \end{pmatrix} = \begin{bmatrix} Z_{11}(B_z) & Z_{12}(B_z) \\ Z_{21}(B_z) & Z_{22}(B_z) \end{bmatrix} \begin{pmatrix} i_1 \\ i_2 \end{pmatrix}. \quad (1)$$

In Eq. (1), $B_z\,(=\mu_0 H_z)$ is the external magnetic induction applied in the wire axis direction, and v_i and i_i are the ac voltage and current appearing across or flowing through the magnetic wire or pickup coil. The indices, i and j, are 1 for the wire and 2 for the coil.

Based on the description of the GMI effect proposed by Ménard and Yelon [12], each term Z_{ij} of the impedance matrix of a uniformly magnetized surface region of a ferromagnetic microwire is given [8] by

$$Z_{11} = \frac{l}{2\pi a}\left(Z_M \cos^2\theta_M + Z_N \sin^2\theta_M\right) \quad (2a)$$

$$Z_{12} = Z_{21} = N\left(Z_N - Z_M\right)\sin\theta_M \cos\theta_M \quad (2b)$$

$$Z_{22} = \frac{2\pi a N^2}{l}\left(Z_M \sin^2\theta_M + Z_N \cos^2\theta_M\right) \quad (2c)$$

where l is the length of the sensing element, a the magnetic wire radius and N the number of turns of the pick-up coil. θ_M is the angle between the magnetization direction and the wire axis direction. This angle is determined from the static equilibrium position which minimizes the free energy density of the system and depends upon the axial applied magnetic field, H_{z0}, the circumferential static magnetic field, $H_{\varphi 0}$ (induced by a static bias current I_{dc} such that $H_{\varphi 0} = \frac{I_{dc}}{2\pi a}$), and the magnitude, H_k, and direction, θ_k, of the anisotropy field. The terms Z_M and Z_N are the magnetic and non-magnetic component of the surface impedance tensor, respectively. They are determined, as given in [8], by the simultaneous solution of Maxwell's equations and the Landau-Lifshitz equation in the magnetic configuration given by the static equilibrium condition. In what follows, we assume that the circumferential excitation field (induced by the ac excitation current) is small compared with the effective internal field, given by

$$H_{int} = H_{z0}\cos\theta_M + H_{\varphi 0}\sin\theta_M + H_k\cos 2(\theta_k - \theta_M). \quad (3)$$

Under these circumstances the amplitude of the ac magnetization will be small compared to the saturation magnetization, M_s. These are the conditions for the linear regime, as specified above.

In the usual set-up, the GMI wire is driven by a high frequency current which induces a voltage at the wire or pick-up coil ends, depending upon the configuration, proportional to the impedance, and reflecting its dependence upon the magnetic field. Assuming that the sensing element is operated in a field closed loop, fed by a sinusoidal driving current of amplitude I_{ac}, the output signal after demodulation is [8] :

$$V_s(t) = k_d I_{ac}\left(Z_{ij_0} + \left.\frac{\partial Z_{ij}(B)}{\partial B}\right|_{B=B_{z0}} b(t) + z_{n_{ij}}(t)\right) + e_n(t). \quad (4)$$

In Eq. (4), B_{z0} is the static working point of the closed loop, $b(t)$, the small signal variation around it, and $Z_{ij_0} = Z_{ij}(B_{z0})$. The term $\partial Z_{ij}(B)/\partial B$ is the intrinsic sensitivity of the sensing element, expressed in units of Ω/T. The factor k_d is the demodulation gain which depends upon the demodulation technique employed and the excitation wave forms. The terms $z_{n_{ij}}(t)$ and $e_n(t)$ are the intrinsic noise, expressed as an equivalent impedance fluctuation, and the output noise from the electronic conditioning circuitry, respectively. Note that, at this point, no assumption has been made as to the frequency behavior of these noise sources. For what follows, it is convenient to define a sensitivity,

$$S = k_d I_{ac}\left.\frac{\partial Z_{ij}(B)}{\partial B}\right|_{B=B_{z0}}, \quad (5)$$

in units of $(\mathrm{V/T})$. We now consider the various contributions to noise, appearing in Eq. (4).

III. Noise Model

A. White noise

As shown previously [8], the output noise level of GMI sensors in the white noise region is dominated by the sources due to the electronic conditioning, and one may neglect the intrinsic noise arising from the sensing element. Thus, this model allows us to predict the white noise component, $e_{n_W}(t)$, of the term $e_n(t)$ in Eq. (4).

The noise sources considered were those which contribute to the high frequency white noise level near the carrier frequency, which are transposed to low frequency by demodulation, in addition to those which appear directly at low frequency. Considering the off-diagonal configuration, a general expression for this white noise spectral density is [8]

$$e_{n_W}^2 = k_{en}^2\left\{G_c^2\left[(Z_{21_0})^2\, i_{n_g}^2 + e_{n_Q}^2\right] + e_{n_f}^2\right\} + e_{n_{LF}}^2. \quad (6)$$

In Eq. (6), i_{n_g} is the white noise arising from the excitation current generator, e_{n_Q} is the noise contribution due to the resistance of the pick-up coil, e_{n_f} represents all wide band noise sources appearing at the demodulation input and $e_{n_{LF}}$ is the low frequency white noise appearing after demodulation. G_c is the total chain gain applied before demodulation and k_{en} is the narrow band noise demodulation gain. We note that both factors, k_{en} and k_d, (this last appearing in Eq. (4)) depend upon the demodulation technique employed and excitation wave forms as discussed in [13].

The equivalent magnetic noise power spectral density of the setup, expressed in T^2/Hz, is obtained as the ratio of the output voltage noise level to the sensitivity

$$b_{n_W}^2 = \frac{e_{n_W}^2}{S^2}. \quad (7)$$

B. Low frequency excess noise

Despite agreement with experimental measurements in the white noise region, the previous model does not include the $1/f$ low frequency excess noise usually observed in measured spectra [4], [5], [6], [7]. Further improvement of GMI based magnetometers requires better understanding of the origins of this noise. As we did for the white noise region, we might assume that the $1/f$ excess noise is due to electronic conditioning circuitry (for example, from the excitation generator or from the input of the demodulation stage). However, cross-correlation measurements suggest that this low frequency excess noise is intrinsic to the sensing element and thus exhibits an intrinsic equivalent magnetic noise [14]. This conclusion is supported by research on the operating state of the sensing element presented in [5], [4], showing that the $1/f$ noise level depends strongly upon the parameters chosen for annealing of the magnetic wire and upon the DC bias current applied to the wire.

As discussed above, we have recently proposed a model in which the low frequency excess noise of GMI may be induced by magnetization fluctuations [11]. This analysis, which relies upon strong simplifying hypotheses, was proposed for the classical GMI case, that is, indices $i, j = 1, 1$ in Eq. (4). We did not consider other two-port network cases, such as off-diagonal GMI. Here, we extend this analysis.

The impedance of the sensing element strongly depends upon its magnetization direction θ_M. That is, any intrinsic fluctuation of the magnetization will potentially induce fluctuations, $z_{n_{ij}}(t)$, of the impedance, Z_{ij}, and set a fundamental

limit to the signal-to-noise ratio of the sensor. The power spectral density of the impedance fluctuations, in units of Ω^2/Hz, is given by

$$z^2_{n_{ij}}(f) = \left(\frac{\partial Z_{ij}}{\partial \theta_M}\right)^2 S_{\theta_M\theta_M}(f), \tag{8}$$

where $S_{\theta_M\theta_M}$ is the power spectral density of the magnetization direction fluctuations (in units of $\mathrm{rad}^2/\mathrm{Hz}$) and $\partial Z_{ij}/\partial\theta_M$ is the dependence of each term of the impedance matrix upon magnetization direction.

Based on the fluctuation-dissipation theorem, as previously described for magnetic tunnel junction sensors [15], CsNiFeF_6 spin glasses [16], Flux-gate sensors [17], and giant magneto resistance sensors [18], the spectral density of magnetization direction fluctuations, $S_{\theta_M\theta_M}$, is expressed by:

$$S_{\theta_M\theta_M}(f) = \frac{4k_BT}{2\pi f V\mu_0 M_s^2}\chi"(f), \tag{9}$$

where k_BT is the thermal energy, $V(=l\pi a^2)$ is the volume of the magnetic wire and $\chi"(f)$ is the imaginary (lossy) part of the complex magnetic susceptibility. The spectral density of the impedance fluctuations, $z_{n_{ij}}$, may then be expressed as an equivalent magnetic noise spectral density after dividing by the intrinsic sensitivity, $\partial Z_{ij}(B)/\partial B$, of the sensor.

Bertotti [19] has investigated the frequency dependence of low frequency losses, and the physical mechanisms at their origin, for a number of relatively soft magnetic metals, particularly transformer steels. An illustration of his observations of the frequency dependence of $\chi"(f)$ is presented in Figure 1. He associates the frequency independent part of $\chi"(f)$ with the area of the irreversible part of the quasi-static hysteresis magnetization cycle, the dependence upon f with magnetization dynamics (so-called "classic" losses), and the dependence upon $\sqrt{f}$ to "excess" losses arising from domain wall motion. From impedance measurements we find that GMI wires usually exhibit similar behavior. Regardless of detailed mechanisms, at very low frequency, $\chi"(f)$ is constant. From Eq. (9) we see that the noise spectral density will vary as $1/f$ until other dissipation mechanisms arise with increasing frequency.

When the ac field amplitude is low enough so that the magnetization is in the linear regime the circumferential hysteresis loop $M_\varphi - H_\varphi$ is an ellipse described by $M_\varphi(t) = \chi H_\varphi(t)$ with $\chi(f) = \chi'(f) - \imath\chi"(f)$, constant for a given value of f. The area, A, of this ellipse is given by integrating M_φ over H_φ yielding

$$A = \pi\chi"(f)H^2_{\varphi a}. \tag{10}$$

where $H_{\varphi a}$ is the amplitude of $H_\varphi(t)$. If the model presented in [11] is correct, we may determine the magnitude of the noise (Eq. (9)), from the area A.

It is important to understand that Eq. (10) is not limited to the linear regime. In the non-linear regime, $M_\varphi(t)$ can be expressed by its Fourier components $M^n_\varphi(t)$ (where n is the harmonic number). And then, only the fundamental harmonic $M^1_\varphi(t) = \chi H_{\varphi a}$ contributes to the surface [20].

A theoretical worst case limit corresponds to the case of a rectangular hysteresis loop without reversible parts where

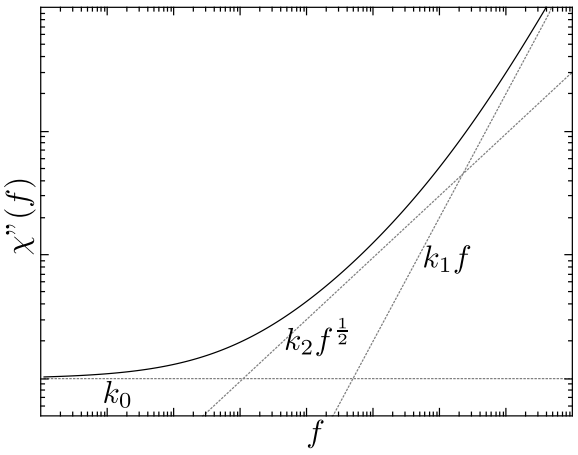

Figure 1: Illustration of the frequency dependence of the imaginary part of the complex susceptibility due to contribution of various dissipation mechanisms. The curve follows a frequency dependence of $\chi"(f) = k_0 + k_1 f + k_2\sqrt{f}$. After [19].

$M_\varphi = \pm M_s$. This case can only be reached when three ideal conditions are satisfied at the same time:

1) The anisotropy is homogeneous and the easy axis is circumferential.
2) The applied dc field $H_{z0} = 0$.
3) The dc circumferential field $H_{\varphi 0} = 0$.

The magnetic susceptibility of the fundamental harmonic of $M_\varphi(t)$ is then given by its real and imaginary parts: $\chi' = 0$ and $\chi" = \frac{4}{\pi}M_s/H_k$. As $H_{\varphi a}$ increases beyond H_k, χ' asymptotically tends to $\frac{4}{\pi}M_s/H_{\varphi a}$ and $\chi"$ asymptotically decreases to zero due to magnetic saturation.

Figure 2 shows an example of comparison between a theoretical worst case loop and a real loop measured when conditions 2 and 3 are satisfied. The measurements are obtained on a 50 μm diameter Co rich amorphous micro-wire, where the hysteresis loop is computed from time integration of the voltage distortions appearing accross the wire submitted to a sine wave excitation current. Two different amplitudes of H_φ/H_k are shown for both real and theoretical cases: a high H_φ/H_k leading to major hysteresis loops and a low H_φ/H_k leading to minor loops.

Because of inhomogeneities of the micro-wire magnetic structure and the ac field inside a micro-wire, the surface of the real hysteresis major loop is smaller than its theoretical value. Nevertheless, the two corresponding values of $\chi"$ (which is proportional to $A/H^2_{\varphi a}$) are of the same order. At lower amplitude of H_φ/H_k, the measured curve is almost elliptical, corresponding to the linear regime. Even in this regime, the surface of the loop is of the order of the worst case one (about a third of the circle surface) so the same ratio is valid for the two corresponding values of $\chi"$. This allows as to write:

$$\chi"(f) \lesssim \frac{M_s}{H_k}. \tag{11}$$

Equation (11) places a pessimistic upper limit upon the noise level, discussed in what follows.

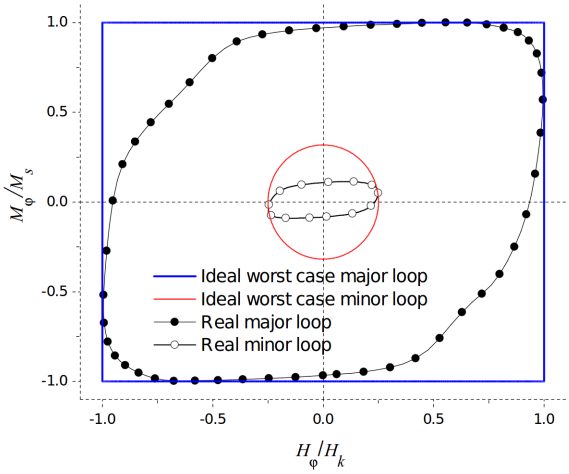

Figure 2: Comparison between a hysteresis loop corresponding to the ideal worst case and examples of real loops measured in worst case conditions. The major ideal loop is rectangular, delimiting a maximum surface. The ideal minor loop is obtained by keeping $A/H_{\varphi a}^2$ ratio of the ideal loops unchanged. This loop is plotted for the sake of comparison between the surface of the worst case loop and the surface of the real minor loop in the linear regime. Here, the measurements are performed at 800 Hz and $H_{z0} = 0$.

1) Noise from magnetization fluctuations in classical GMI: An analytical expression of the term $\partial Z_{ij}/\partial\theta_M$, appearing in Eq. (8) was derived for the classical GMI setup, from the expression for Z_{11} in Eq. (1), and proposed, by Melo *et al.* [21], to be

$$\frac{\partial Z_{11}}{\partial\theta_M} = \frac{l}{2\pi a} Z_N \left\{ -\frac{\xi}{2M_s}\sqrt{\mu_t^3}\left[\frac{3H_k}{2}\sin\left(2\theta_k - 2\theta_M\right) - H_{int}\cot\theta_M\right]\cos^2\theta_M - \xi\left(\mu_t - 1\right)\sin(2\theta_M)\right\}. \quad (12)$$

In Eq. (12), the parameter ξ is a function of the wave vectors in the magnetic material appearing in the expression for Z_M [21], and $\mu_t \approx M_s/H_{int}$ for excitation frequencies well below that of ferromagnetic resonance. We recall here that H_{int} is given by Eq. (3).

2) Extension to the off-diagonal configuration: Extending the previous noise source to the off-diagonal configuration relies only upon the sensitivity of the term Z_{21} of the impedance matrix to the magnetization direction. In our case, the quantity of interest is the equivalent magnetic noise spectral density, in units of $\mathrm{T}/\sqrt{\mathrm{Hz}}$, induced by the magnetization fluctuations, given by

$$b_{n_I}(f) = z_{n_{ij}}(f)/\left(\frac{\partial Z_{ij}}{\partial B}\right). \quad (13)$$

As discussed in [21], the intrinsic sensitivity of the sensing element may be expressed as

$$\frac{\partial Z_{ij}}{\partial B} = \frac{\partial Z_{ij}}{\partial\theta_M}\frac{\partial\theta_M}{\partial B} = -\frac{\partial Z_{ij}}{\partial\theta_M}\frac{\sin\theta_M}{\mu_0 H_{int}}. \quad (14)$$

Combining Eqs. (8), (9), (13) and (14) leads to an expression for the equivalent magnetic noise power spectral density induced by magnetization fluctuations

$$b_{n_I}^2(f) = \frac{\mu_0}{\sin^2\theta_M}\frac{4k_BT}{2\pi fV}\frac{H_{int}^2}{M_s^2}\chi"(f). \quad (15)$$

We see that Eq. (15) does not depend upon the specific term of the impedance matrix for which it was calculated. This highlights the fact that the intrinsic noise behaves like a magnetic signal sensed by the sensor, with no dependence upon its sensitivity. In other words, magnetic voltage noise scales with sensitivity, leading to a sensitivity independent equivalent magnetic noise. Nevertheless, we must recall here that this noise will be measurable only in the operating mode (off-diagonal GMI) for which the sensitivity is high enough for this noise to rise above the equivalent magnetic white noise floor due to electronic conditioning circuitry.

It is also notable that this noise level depends only upon the magnetization direction angle, θ_M, defined by the static equilibrium condition. That is, we are then able to perform numerical simulations, based on general equations of the GMI effect, which determine the intrinsic low frequency excess noise level as a function of the static working point (both axial and circumferential magnetic field) and the effective anisotropy.

As an example, assuming a wire with a circumferential anisotropy and a zero static bias current ($H_{\varphi 0} = 0$), the magnetization as a function of field is given by $M/M_s = \cos\theta_M = H_{z0}/H_k$ and the internal stiffness field by $H_{int} = (H_k^2 - H_{z0}^2)/H_k$. Considering a static working point approximately equal to $H_{z0} = H_k/2$ which maximizes the sensitivity, Eq. (15) yields

$$b_{n_I}^2(f) \lesssim \frac{3\mu_0 k_BT}{\pi fV}\frac{H_k}{M_s}. \quad (16)$$

IV. Results and Discussion

Based upon the model described here, we have studied the low frequency excess noise behavior of a working GMI magnetometer, taking into account the white noise induced by the electronic conditioning circuitry and the sensing element sensitivity. Now, we consider the conditioning circuitry described in [8] based on sine wave current excitation and peak detector demodulation. The sensing element itself consists of a GMI wire referred to as c3 in [22] associated with a 600 turn pick-up coil. For such a wire, the following parameters are considered: $H_k = 40\,\mathrm{A/m}$, $M_s = 560\,\mathrm{kA/m}$, $l = 3\,\mathrm{cm}$, and $a = 50\,\mu\mathrm{m}$.

The predicted noise is a function of the applied magnetic field. Generally, the sensor is operated under a field locked loop in its most sensitive range, which roughly matches the range of maximum slope in the low field region ($|B_{z0}| \lesssim 50\,\mu\mathrm{T}$ in our case), leading to sensitivity values such as $\frac{\partial Z_{11}}{\partial B} \approx 400\,\mathrm{k\Omega/T}$ and $\frac{\partial Z_{21}}{\partial B} \approx 1.77\,\mathrm{M\Omega/T}$. Here, it is important to note that the sensitivity outside the central low field region is clearly overestimated by the model, as compared to measured impedance variations.

Figure 3a shows the white noise level behavior for a given static working point for classical GMI and for off-diagonal

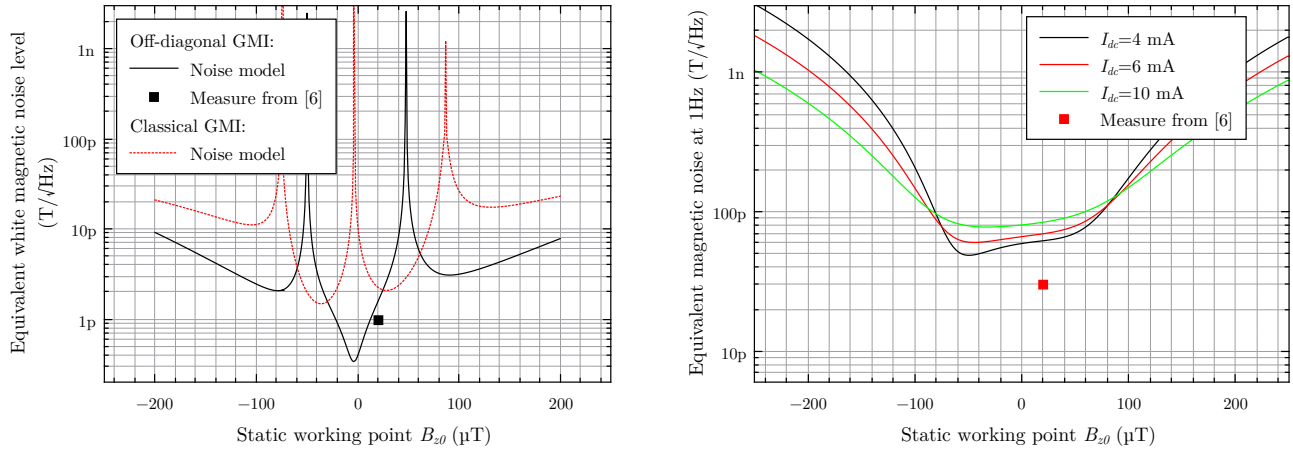

(a) (b)

Figure 3: Equivalent magnetic noise level, expressed as $\mathrm{T}/\sqrt{\mathrm{Hz}}$, versus applied magnetic field, assuming the following parameters: $H_k = 40\,\mathrm{A/m}$, $\theta_k = 85°$, $M_S = 560\,\mathrm{kA/m}$, $l = 3\,\mathrm{cm}$, $a = 50\,\mu\mathrm{m}$, excitation frequency $f_p = 1\,\mathrm{MHz}$, coil turns, $N = 600\,\mathrm{turns}$, and considering the operating setup conditions presented in [8]. The curve in (a) are the white noise levels induced by electronic conditioning circuitry in classical and off-diagonal GMI configurations, assuming a DC bias current of $I_{dc} = 6\,\mathrm{mA}$, calculated from Eq. (7). The curves in (b) represent the low-frequency intrinsic excess noise level at 1 Hz, for several DC bias currents, calculated from Eq. (15) assuming the pessimistic upper limit for $\chi"(f) = M_s/H_k = 14000$. Square dots represent the measured values of the equivalent magnetic noise in the white noise region (a) and at 1 Hz (b) in the off-diagonal configuration from [6].

GMI. These predicted performances are in fair agreement with those measured in the central low field area of about $1\,\mathrm{pT}/\sqrt{\mathrm{Hz}}$ as presented in [6]. Nevertheless, the noise level should be higher in the external area, due to the overestimation of the sensitivity.

The excess noise level at 1 Hz is evaluated by fixing $f = 1$ Hz in Eq. (15), which predicts a $1/f$ behavior, and using our pessimistic upper limit for $\chi"(f)$. The solid lines in Fig. 3b show the noise level at 1 Hz as a function of the static working point B_{z0}, for several DC bias currents. We recall here that this noise level is the same for all configurations of the sensing two-port network. Nevertheless, the choice of configuration will determine the sensor sensitivity, given by Eq. (5) as well as the noise level arising from electronic conditioning which may be much larger than the intrinsic noise level, shown in Fig. 3. This predicted result is in fair agreement with that measured [6] of about $30\,\mathrm{pT}/\sqrt{\mathrm{Hz}}$ at 1 Hz. This experimental value could be fitted by Eq. (15) using a value of $\chi"(f) \approx 1500$ to be compared to the one obtained from the worst case scenario $\chi"(f) = M_s/H_k = 14000$.

V. Conclusion

We have proposed an extension of the low frequency excess noise model which takes into account the off-diagonal two-port configuration. The model clearly yields the $1/f$ behavior of the measured noise spectrum as long as the imaginary part of the complex magnetic susceptibility is independent of the frequency, which is the case for the low frequency range in which dissipation is governed by quasi-static hysteretic losses. We find, notably, that, regardless of the element of the two-port network sensor which is measured, magnetization fluctuations induce a similar level of equivalent magnetic noise. Thus, the low-frequency excess noise will be measurable only for the operating mode which minimizes the equivalent magnetic white noise level. Further, magnetic noise depends strongly upon the static equilibrium condition, which is governed by the effective anisotropy of the magnetic wire and both axial and circumferential static working point. That is, it could be used to deduce the optimized working conditions for the sensing element.

The general approach of magnetization fluctuations should be applicable in principle to other GMI sensing element such as electroplated tube or multilayers. However, while similar general conclusions should be reached for such elements, a quantitative noise predictions would require models to estimate the sensitivity.

Furthermore, effects of both axial and circumferential static working point on the values of $\chi"(f)$ have not been considered here. Despite this, we may expect that the static working condition, that is dc axial magnetic field and dc bias current, should affect fluctuations of the magnetization direction. Indeed, in order to minimize the magnitude of the excess noise at 1 Hz, it is necessary to obtain low values of the imaginary part of the complex magnetic susceptibility. This factor depends upon several working condition parameters such as the excitation frequency and the ratio between static and excitation current amplitude, and is the subject of current investigation [5], [4]. Thus, a more complete model, which should also include non-linear aspects of the GMI effect as presented in [23], would be of great interest.

REFERENCES

[1] M. Knobel, M. Vázquez, and L. Kraus, "Giant magnetoimpedance," *Handbook of Magnetic Materials*, vol. 15, pp. 1–92, 2003.

[2] L. V. Panina, K. Mohri, K. Bushida, and M. Noda, "Giant magneto-impedance and magneto-inductive effects in amorphous alloys (invited)," *Journal of Applied Physics*, vol. 76, no. 10, p. 6198, 1994.

[3] T. Uchiyama, K. Mohri, L. Panina, and K. Furuno, "Magneto-impedance in sputtered amorphous films for micro magnetic sensor," *IEEE Transactions on Magnetics*, vol. 31, no. 6, pp. 3182–3184, 1995.

[4] M. Butta, S. Yamashita, and I. Sasada, "Reduction of Noise in Fundamental Mode Orthogonal Fluxgates by Optimization of Excitation Current," *IEEE Transactions on Magnetics*, vol. 47, no. 10, pp. 3748–3751, Oct. 2011.

[5] M. Butta and I. Sasada, "Sources of Noise in a Magnetometer Based on Orthogonal Fluxgate Operated in Fundamental Mode," *IEEE Transactions on Magnetics*, vol. 48, no. 4, pp. 1508–1511, Apr. 2012.

[6] B. Dufay, S. Saez, C. Dolabdjian, A. Yelon, and D. Ménard, "Development of a High Sensitivity Giant Magneto-Impedance Magnetometer: Comparison With a Commercial Flux-Gate," *IEEE Transactions on Magnetics*, vol. 49, no. 1, pp. 85–88, Jan. 2013.

[7] E. Fernández, A. García-Arribas, J. M. Barandiarán, A. V. Svalov, G. V. Kurlyandskaya, and C. P. Dolabdjian, "Equivalent Magnetic Noise of Micro-Patterned Multilayer Thin Films Based GMI Microsensor," *IEEE Sensors Journal*, vol. 15, no. 11, pp. 6707–6714, 2015.

[8] B. Dufay, S. Saez, C. Dolabdjian, A. Yelon, and D. Ménard, "Characterization of an Optimized Off-Diagonal GMI-Based Magnetometer," *IEEE Sensors Journal*, vol. 13, no. 1, pp. 379–388, Jan. 2013.

[9] S. Sandacci, D. Makhnovskiy, L. Panina, K. Mohri, and Y. Honkura, "Off-Diagonal Impedance in Amorphous Wires and Its Application to Linear Magnetic Sensors," *IEEE Transactions on Magnetics*, vol. 40, no. 6, pp. 3505–3511, Nov. 2004.

[10] E. Paperno, "Suppression of magnetic noise in the fundamental-mode orthogonal fluxgate," *Sensors and Actuators A: Physical*, vol. 116, no. 3, pp. 405–409, Oct. 2004.

[11] C. Dolabdjian, B. Dufay, S. Saez, A. Yelon, and D. Ménard, "Is Low Frequency Excess Noise of GMI Induced by Magnetization Fluctuations?" *Key Engineering Materials*, vol. 605, pp. 437–440, Apr. 2014.

[12] D. Ménard and A. Yelon, "Theory of longitudinal magnetoimpedance in wires," *Journal of Applied Physics*, vol. 88, no. 1, p. 379, 2000.

[13] L. Ding, S. Saez, and C. Dolabdjian, "Low Frequency Giant Magnetoimpedance Magnetometer Noise Versus Electronic Conditioning," *Sensor Letters*, vol. 5, no. 1, pp. 248–251, Mar. 2007.

[14] E. Portalier, B. Dufay, S. Saez, and C. Dolabdjian, "Étude du bruit excédentaire a basse fréquence dans les magnetomètres a base de Magneto-Impedance Géante (MIG)." Assemblé générale "Interférences d'Ondes", 19 Oct. 2015.

[15] W. F. Egelhoff, P. W. T. Pong, J. Unguris, R. D. McMichael, E. R. Nowak, a. S. Edelstein, J. E. Burnette, and G. a. Fischer, "Critical challenges for picoTesla magnetic-tunnel-junction sensors," *Sensors and Actuators, A: Physical*, vol. 155, no. 2, pp. 217–225, 2009.

[16] P. Refregier and M. Ocio, "Measurement of spontaneous magnetic fluctuations," *Rev. Phys. Appl*, vol. 22, no. 5, pp. 367–374, 1987.

[17] R. H. Koch, J. G. Deak, and G. Grinstein, "Fundamental limits to magnetic eld sensitivity of uxgate magnetic eld sensors," *Appl. Phys. Lett.*, vol. 10598, no. 75, p. 3862, 1999.

[18] N. Smith and P. Arnett, "White-noise magnetization fluctuations in magnetoresistive heads," *Applied Physics Letters*, vol. 78, no. 10, pp. 1448–1450, 2001.

[19] G. Bertotti, "General Properties of Power Losses in Soft Ferromagnetic Materials," *IEEE Transactions on Magnetics*, vol. 24, no. 1, pp. 621–630, 1987.

[20] G. Bertotti, *Hysteresis in Magnetism: For Physicists, Materials Scientists, and Engineers*. Academic Press, 1998.

[21] L. G. C. Melo, D. Ménard, A. Yelon, L. Ding, S. Saez, and C. Dolabdjian, "Optimization of the magnetic noise and sensitivity of giant magnetoimpedance sensors," *Journal of Applied Physics*, vol. 103, no. 3, p. 033903, 2008.

[22] B. Dufay, S. Saez, C. Dolabdjian, A. Yelon, and D. Ménard, "Physical properties and giant magnetoimpedance sensitivity of rapidly solidified magnetic microwires," *Journal of Magnetism and Magnetic Materials*, vol. 324, no. 13, pp. 2091–2099, Jul. 2012.

[23] D. Seddaoui, D. Ménard, B. Movaghar, and A. Yelon, "Nonlinear electromagnetic response of ferromagnetic metals: Magnetoimpedance in microwires," *Journal of Applied Physics*, vol. 105, no. 8, p. 083916, 2009.